

# Exact expressions for correlations in the ground state of the dense $O(1)$ loop model

S Mitra<sup>1</sup>, B Nienhuis<sup>1</sup>, J de Gier<sup>2</sup> and M T Batchelor<sup>3</sup>

<sup>1</sup> Instituut voor Theoretische Fysica, Universiteit van Amsterdam,  
1018 XE Amsterdam, The Netherlands

<sup>2</sup> Department of Mathematics and Statistics, The University of Melbourne,  
VIC 3010, Australia

<sup>3</sup> Department of Theoretical Physics, Research School of Physical Sciences and  
Engineering and Mathematical Sciences Institute, Australian National  
University, Canberra ACT 0200, Australia

E-mail: [saibalm@science.uva.nl](mailto:saibalm@science.uva.nl), [nienhuis@science.uva.nl](mailto:nienhuis@science.uva.nl),  
[degier@ms.unimelb.edu.au](mailto:degier@ms.unimelb.edu.au) and [murrayb@maths.anu.edu.au](mailto:murrayb@maths.anu.edu.au)

Received 24 July 2004

Accepted 17 September 2004

Published 30 September 2004

Online at [stacks.iop.org/JSTAT/2004/P09010](http://stacks.iop.org/JSTAT/2004/P09010)

doi:10.1088/1742-5468/2004/09/P09010

**Abstract.** Conjectures for analytical expressions for correlations in the dense  $O(1)$  loop model on semi-infinite square lattices are given. We have obtained these results for four types of boundary conditions. Periodic and reflecting boundary conditions have been considered before. We give many new conjectures for these two cases and review some of the existing results. We also consider boundaries on which loops can end. We call such boundaries ‘open’. We have obtained expressions for correlations when both boundaries are open, and one is open and the other one is reflecting. Also, we formulate a conjecture relating the ground state of the model with open boundaries to fully packed loop models on a finite square grid. We also review earlier obtained results about this relation for the three other types of boundary conditions. Finally, we construct a mapping between the ground state of the dense  $O(1)$  loop model and the  $XXZ$  spin chain for the different types of boundary conditions.

**Keywords:** integrable spin chains (vertex models), loop models and polymers, solvable lattice models

---

**Contents**

<b>1. Introduction</b>	<b>2</b>
<b>2. The dense <math>O(n)</math> loop model</b>	<b>3</b>
<b>3. The Hamiltonian and the transfer matrix</b>	<b>5</b>
<b>4. Components of the ground state</b>	<b>7</b>
4.1. Periodic and reflecting boundary conditions . . . . .	9
4.2. Open and mixed boundary conditions . . . . .	11
<b>5. Correlations and exponents</b>	<b>12</b>
<b>6. Fully packed loop diagrams</b>	<b>14</b>
<b>7. Interpretation as families of nonintersecting lattice paths</b>	<b>17</b>
<b>8. Mapping loop model <math>\rightarrow</math> ground state of <math>XXZ</math> model</b>	<b>19</b>
8.1. Open and mixed boundary conditions . . . . .	21
<b>9. Conclusion</b>	<b>22</b>
<b>Acknowledgments</b>	<b>22</b>
<b>Appendix. The boundary term</b>	<b>23</b>
<b>References</b>	<b>24</b>

---

**1. Introduction**

Recently Razumov and Stroganov [1, 2] made some remarkable observations concerning the ground state of the antiferromagnetic  $XXZ$  quantum chain of odd, finite length and with periodic boundary conditions, and with anisotropy parameter  $\Delta = -1/2$ . The ground state vector expressed in the standard basis of spin configurations relative to the  $z$ -axis has all positive elements. If these elements are normalized such that the smallest element is unity, all elements turn out to have integer values. The most striking observation is that some combinations of these integers are related to the number of alternating sign matrices (ASMs) [5, 6]. These are matrices of which the elements are equal to 0, 1 or  $-1$ , the nonzero elements alternate in sign and in each row and each column the elements add up to 1.

Since the first paper in the subject the relation between the  $XXZ$  chain and the ASM has been extended considerably. It was noted [8] that the relation is more generic if the  $XXZ$  Hamiltonian is reformulated in a different form, that of a dense loop model. This form is based on a well known equivalence [22] between the  $Q$ -state Potts model at its critical point [23], the dense loop model and the six-vertex model. Of these two-dimensional statistical models the transfer matrix can be taken to the limit of extreme spatial anisotropy where it takes a simpler form which can be written as the quantum Hamiltonian. This relates the six-vertex model to the  $XXZ$  chain, and the equivalent dense loop model to a Hamiltonian acting on configurations of arcs that connect pairwise

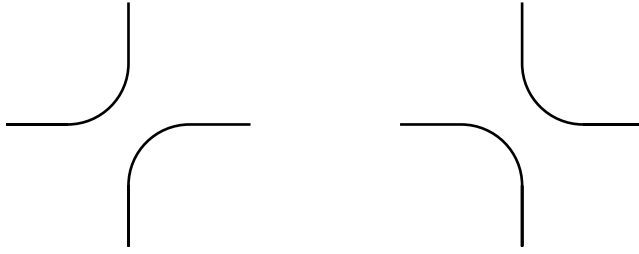


**Figure 1.** The two vertices of the dense  $O(1)$  loop model.

the sites of a chain. This loop Hamiltonian can be expressed neatly in a graphical representation of the Temperley–Lieb algebra [9, 10].

It is in this formulation that the original authors [3] discovered that the connection between the ground state of the loop Hamiltonian and the ASM is considerably more detailed. This is based in part on a simple bijection between the class of ASMs and the configurations of fully packed loop (FPL) models on a finite square grid with specific boundary conditions. It turns out that each element of the ground state vector of the loop Hamiltonian is equal to the cardinality of a well defined subset of FPL configurations. It turns out (see [4] and [9]) that different boundary conditions of the loop Hamiltonian translate into different symmetry classes of FPL configurations. A review of these results has been presented by de Gier [11].

In this paper we generalize these results to other boundary conditions than have been considered so far. It is remarkable how robust the results are under this type of variation. Also, we give explicit expressions for several classes of elements of the ground state vector as well as for classes of correlation functions. We also solve the reflection equation for the random cluster model, which underlies the Hamiltonian for other than periodic boundary conditions. Finally, in order to make connection with the  $XXZ$  chain we give an explicit transformation for vectors and operators in the loop representation to the spin representation.

## 2. The dense $O(n)$ loop model

The states of the dense  $O(n)$  loop model [21] are graphs consisting of nonintersecting closed loops covering all the edges of the lattice. Each vertex is visited twice. Vertices can thus be in two states as shown in figure 1.

The Boltzmann weight of a state consisting of  $l$  loops is  $n^l$ . At  $n = 1$  all configurations are equally likely. At this point the model can be mapped to the bond percolation problem at criticality, the six-vertex model and the  $XXZ$ -spin chain at  $\Delta = -1/2$  (see [22] and section 8). The corresponding bond percolation problem is defined on one of the sublattices of the dual lattice. The states of the dense  $O(1)$  loop model are in direct bijection with bond configurations of the bond percolation problem; see figure 2.

In this paper we will focus on the dense  $O(1)$  loop model on an  $L \times \infty$  lattice subjected to the following boundary conditions.

- Periodic: the topology of the lattice is that of a cylinder.

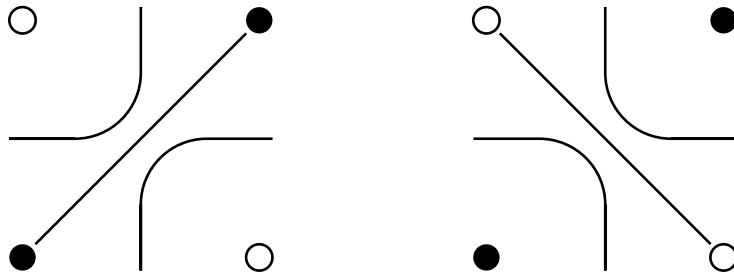


**Figure 2.** The mapping of a loop configuration to a bond configuration of the corresponding bond percolation problem. A bond is either put on an edge of the square lattice formed by the  $\bullet$  or on the dual edge orthogonal to it on the square lattice formed by the  $\circ$ .

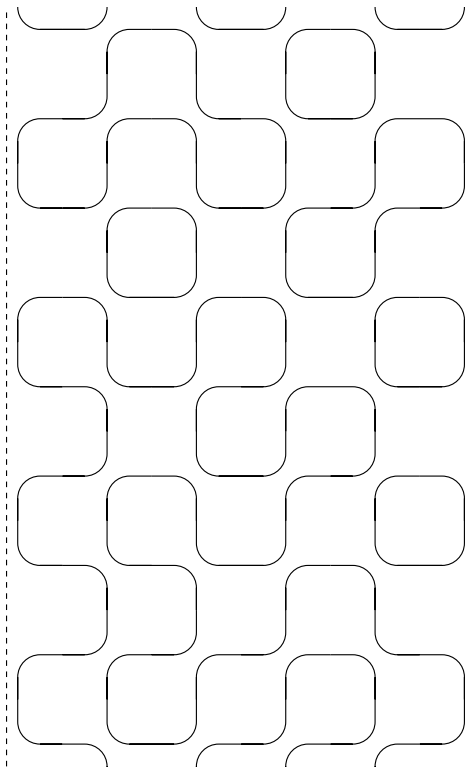


**Figure 3.** Part of a typical configuration of the  $O(1)$  loop model on a  $6 \times \infty$  strip with reflecting boundaries.

- Reflecting: at the boundaries the edges of even rows that end on the boundary are connected to those of the odd row above it as indicated in figure 3.
- Mixed: loops can end at the left boundary, while at the right boundary reflecting boundary conditions are imposed.
- Open: loops can end at both boundaries.

A horizontal cut between the vertices will intersect the loops at  $L$  points. We define the connectivity state of the cut as the way these  $L$  points are connected to each other or

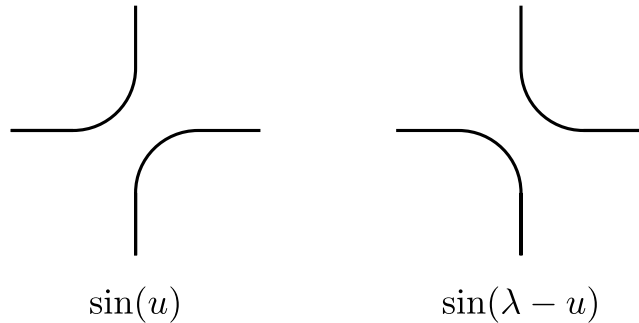


**Figure 4.** Boltzmann weights for a commuting set of transfer matrices.

to the boundary by the loops via the half space below the cut. We will conjecture exact expressions for certain classes of connectivity states. Correlations can be defined as the probability that a subset of the points are connected in a prescribed way. We will also conjecture exact expressions for some correlations. Connectivity states can be represented by a string of parentheses. If a point at position  $i$  is connected to a point at position  $j$ , then this is represented by a parenthesis at position  $i$  matching with a parenthesis at position  $j$ . If the point is connected to the left or right boundary, then that is indicated by a ‘)’ or ‘(’ respectively that does not match with any other parenthesis. If a point is not connected to any other point or to one of the boundaries then that is denoted by a ‘|’.

The expression  $(\dots)_k$  will stand for  $((\dots))_k$ , where  $k$  delimiters have been opened and closed, and the dots symbolize an arbitrary well nested configuration. For instance  $((()))$  will be denoted as  $()_3$ , and  $((()((())))$  will be denoted as  $((())_2)_2$ . We will omit subscripts equal to 1. With a superscript we will denote a repeated concatenation of a structure with itself. E.g.  $()_2^k$  stands for a sequence of  $k$   $()_2$ :  $()_2()_2 \dots$ . Superscripts equal to 1 will be omitted. We will use the following notation for sequences of unpaired delimiters. By  $)_k$  we denote a sequence of  $k$  ‘)’, and by  $(_k$  we denote a sequence of  $k$  ‘(’. Note that we always put the subscript to the right of the delimiter. A configuration of the form  $(\dots)_m$  will be referred to as an  $m$ -nest. Note that an  $m$ -nest with no structure inside it spans  $2m$  points. An  $m$ -nest of this size will be referred to as a minimal  $m$ -nest. An  $m$ -nest spanning the entire system will be referred to as a maximal  $m$ -nest.

### 3. The Hamiltonian and the transfer matrix

When we consider a cut through an infinite strip or cylinder, the probability distribution of specific connectivities at the cut is precisely the distribution found in the eigenvector with the largest eigenvalue.

As usual in integrable systems the transfer matrix is a member of a family of commuting operators parametrized by a spatial anisotropy. This anisotropy is introduced by giving different weights to the two possible vertices of figure 1. In figure 4 they are given the weight  $\sin u$  and  $\sin(\lambda - u)$ , where  $\lambda$  is related to the weight of a loop  $n = 2 \cos \lambda = (q + q^{-1})$ . Eventually, we will set  $\lambda = \pi/3$ , or equivalently  $q = e^{\pi i/3}$ , in order to have  $n = 1$ , but the discussion in this section will be for general  $\lambda$ .

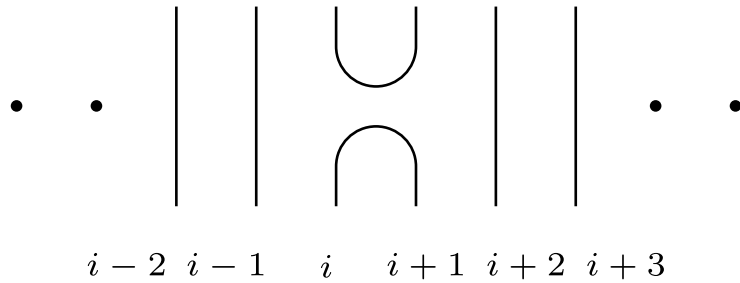


**Figure 5.** The operators  $e_i$ .

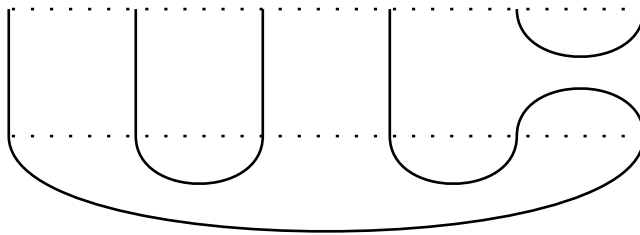


**Figure 6.** The action of  $e_5$  on  $((()))$  resulting in  $({}_2())$ .

The Hamiltonian is now defined as the logarithmic derivative of the transfer matrix

$$H = \frac{1}{T(0)} \left. \frac{dT(u)}{du} \right|_{u=0}. \quad (1)$$

Up to an overall additive and a multiplicative constant the Hamiltonian can be written as

$$H = \sum_{i=1}^L (1 - e_i) \quad (2)$$

where the operators  $e_i$  generate the Temperley–Lieb algebra [24]

$$\begin{aligned} e_j^2 &= (q + q^{-1})e_j \\ e_j e_{j\pm 1} e_j &= e_j \\ e_j e_k &= e_k e_j \quad |j - k| > 1. \end{aligned} \quad (3)$$

The action of the  $e_i$  can be represented graphically as shown in figure 5.

In this graphical notation, the component of the state vector is determined by how the top row of line ends are connected by the figure below it. The action of an operator is visualized by placing the graph of the operator above the graph of the state vector and keeping only the information on how the top row of lines is connected. See figure 6 for an example. Each closed loop gives an overall factor of  $(q + q^{-1})$ .

The Hamiltonian (2) is valid for the periodic system with an additional algebraic relation among the  $e_i$  [27, 28] to ensure that loops winding around the cylinder are treated in the same way as contractible loops. When the loop model is placed on a strip rather than a cylinder, the Hamiltonian is found as the logarithmic derivative of a family of commuting double-row transfer matrices. In the appendix we calculate the form of this

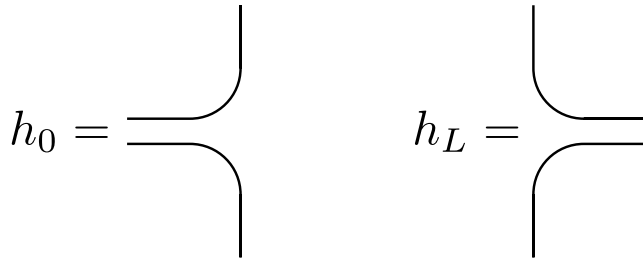


**Figure 7.** Graphical definition of the operators  $h_0$  and  $h_L$ .

double-row transfer matrix from the requirement that the boundary element satisfies the reflection equation [25]. There turns out to be a continuous family of boundary weights that satisfies the reflection equation. In the Hamiltonian limit they add to the TL algebra a left (right) boundary element  $h_0$  ( $h_L$ ) which connects the leftmost (rightmost) line to the boundary, as in figure 7.

These elements satisfy

$$\begin{aligned} h_0^2 &= h_0 & e_1 h_0 e_1 &= e_1 \\ h_L^2 &= h_L & e_{L-1} h_L e_{L-1} &= e_{L-1}. \end{aligned} \quad (4)$$

The coefficient with which they appear in the Hamiltonian is arbitrary, and we choose to consider the following cases: closed or reflecting boundary conditions

$$H = \sum_{i=1}^{L-1} (1 - e_i), \quad (5)$$

open boundary conditions

$$H = 1 - h_0 + \sum_{i=1}^{L-1} (1 - e_i) + 1 - h_L, \quad (6)$$

and mixed boundary conditions

$$H = 1 - h_0 + \sum_{i=1}^{L-1} (1 - e_i). \quad (7)$$

#### 4. Components of the ground state

The lowest eigenvalue of each of the Hamiltonians defined in (2), (5)–(7) is zero for any value of  $L$ , and its corresponding eigenvector possesses some intriguing properties. In this section we give conjectured analytical expressions for certain classes of components of the eigenvector and also for certain classes of correlations. With the exception of a few simple cases, no proofs are available, although some progress in this direction has been made recently [13]. We have computed the eigenvector up to  $L = 18$  for periodic boundaries, up to  $L = 16$  for closed boundaries, up to  $L = 9$  for mixed boundaries and up to  $L = 8$  for open boundaries. We have normalized the eigenvector such that all components are integers with greatest common divisor 1. Guessing analytical expressions

for components amounts to guessing integer sequences from the first few terms. There is no general practical method to do this, unless the sequence is given as a product of a rational function of degree one or a product of such products and so on, recursively. In such cases factorizing the numbers in the sequence will yield only small primes. If it is found that the first few integers in a sequence do indeed factor into small primes, then this is a strong indication that the sequence is of the above type. To find a formula of such a sequence one can transform the original sequence to one that is given as a rational function by applying a transformation  $T$  to the sequence  $a_n$ , defined as

$$T[a_n] = \frac{a_{n+1}}{a_n} \quad (8)$$

often enough [30]. Given enough terms, this method will always succeed. In practice one can often guess such sequences by simply inspecting the prime factorization of the terms in the sequence, even if the above method fails due to a lack of terms. For sequences that do not factor into small primes one can consult a database of integer sequences [29].

The following functions enumerating various symmetry classes of alternating sign matrices will occur frequently in our expressions: the number of  $n \times n$  alternating sign matrices  $A(n)$  [17, 15],

$$A(n) = \prod_{j=0}^{n-1} \frac{(3j+1)!}{(n+j)!} \quad (9)$$

the number of  $2n \times 2n$  half turn invariant alternating sign matrices [14],

$$A_{\text{HT}}(2n) = 2 \prod_{k=1}^{n-1} \frac{3(3k+2)!(3k-1)!k!(k-1)!}{4(2k+1)!^2(2k-1)!^2} \quad (10)$$

the conjectured number of  $(2n-1) \times (2n-1)$  half turn invariant alternating sign matrices [16],

$$A_{\text{HT}}(2n-1) = \prod_{j=1}^{n-1} \frac{4(3j)!^2 j!^2}{3(2j)!^4} \quad (11)$$

the number of  $(2n+1) \times (2n+1)$  vertically symmetric alternating sign matrices [14],

$$A_{\text{V}}(2n+1) = \prod_{i=0}^{n-1} \frac{(3i+2)(6i+3)!(2i+1)!}{(4i+2)!(4i+3)!} \quad (12)$$

the number of cyclically symmetric transpose complement plane partitions in a  $(2n) \times (2n) \times (2n)$  box [18],

$$N_{\text{S}}(2n) = \prod_{i=0}^{n-1} \frac{(3i+1)(6i)!(2i)!}{(4i)!(4i+1)!} \quad (13)$$

and the conjectured number of  $(4n \pm 1) \times (4n \pm 1)$  alternating sign matrices symmetric about both the horizontal and vertical axis [16],

$$A_{\text{HV}}(4n \pm 1) = N_{\text{S}}(2n)A_{\text{V}}(2n \pm 1). \quad (14)$$

Some of the above combinatorial functions are special cases of the functions  $R(n, p)$  and  $Q(n, p)$  defined below. We first define the auxiliary function:

$$d(n) = \prod_{k=1}^{n-1} (2k-1)!! 2^{\lfloor k/2 \rfloor}. \quad (15)$$

$Q(n, p)$  and  $R(n, p)$  are defined as

$$Q(n, p) = d(n)^{-1} \left[ \prod_{k=1}^{(n+1)/3} \prod_{j=3k-n}^{(n+3-3k)/2} (p-j) \right] \left[ \prod_{k=1}^{n/3} \prod_{j=3k-2n}^{-(n+3k)/2} (2p+2j-1) \right] \quad (16)$$

$$R(n, p) = d(n)^{-1} \left[ \prod_{k=1}^{(n+1)/3} \prod_{j=3k-2n-1}^{(1-n-3k)/2} (p+j) \right] \left[ \prod_{k=1}^{n/3} \prod_{j=1-n+3k}^{(2+n-3k)/2} (2p-2j+1) \right]. \quad (17)$$

The following relations hold:

$$\begin{aligned} (A(n))^2 &= Q(n, 2n+1) \\ A(n-1)A(n-2) &= Q(n, 2n-2) \\ A_{\text{HT}}(2n) &= Q(n+1, 2n+1) \\ A_{\text{HT}}(2n+1) &= Q(n+1, 2n+2) \\ A_{\text{V}}(2n+1) &= R(n, 2n+1) \\ N_8(2n) &= R(n, 2n). \end{aligned} \quad (18)$$

#### 4.1. Periodic and reflecting boundary conditions

The smallest components for even periodic and even reflecting systems are maximal  $L/2$  nests. For odd periodic and odd reflecting systems the smallest components are maximal  $L/2$  nests concatenated with an unpaired line. We normalize the eigenvector by putting these components equal to one. We conjecture that with this normalization all components are integers. For some components analytic expressions have been found. These components are listed in table 1.

In [8] the following conjectures were made concerning the largest components and the sum of all components of periodic and reflecting systems. For even periodic and reflecting systems the largest component is a sequence of  $L/2$  minimal one-nests  $(\ )^{L/2}$ . Its value is conjectured to be  $A_{\text{HT}}(L-1)$  for periodic systems and  $N_8(L)$  for reflecting systems. For odd periodic and reflecting systems the largest component is a sequence of  $(L-1)/2$  minimal one-nests, concatenated with an unpaired line,  $(\ )^{\lfloor (L-1)/2 \rfloor}$ . Its value is  $A((L-1)/2)^2$  for periodic systems and  $A_{\text{V}}(L)$  for reflecting systems. The sum of all components of the eigenvector for periodic systems has been conjectured to be  $A_{\text{HT}}(L)$ ; for even reflecting systems this has been conjectured to be  $A_{\text{V}}(L+1)$ , and for odd reflecting systems this has been conjectured to be  $N_8(L+1)$ . We conjecture that two minimal nests side by side inside a maximal nest are given by certain (summations over) binomial determinants.

**Table 1.** Components of the eigenvector for periodic and reflecting boundary conditions. Where necessary, an e or o in the second column indicates if the system size is even or odd.

Component	Periodic	Reflecting
$()_{L/2}$	1	1
$()_{L/2} $	1	1
$()^{L/2}$	$A_{\text{HT}}(L-1)$	$N_8(L)$
$()^{L/2} $	$A\left(\frac{L-1}{2}\right)^2$	$A_V(L)$
$(()^n)_{(L/2)-n}$	$Q(n, L)$	$R(n, L)$
$(()^n)_{((L-1)/2)-n} $	$Q(n, L)$	$R(n, L)$
$(()_s)_t)_{(L/2)-s-t}$	See (21)	See (22)–(24)
$\sum \dots \dots$	e $A_{\text{HT}}(L)$	$A_V(L+1)$
$\sum \dots \dots$	o $A_{\text{HT}}(L)$	$N_8(L+1)$
$\sum \dots (\dots)_m$	$Q\left(\frac{L}{2} - m, L+1\right)$	$R\left(\frac{L}{2} - m, L+1\right)$
$\sum \dots (\dots)_m $	$Q\left(\frac{L-1}{2} - m, L+1\right)$	$R\left(\frac{L-1}{2} - m, L+1\right)$
$\sum \dots \dots () \dots$	e $\frac{3}{8} \frac{L^2}{L^2-1} A_{\text{HT}}(L)$	See (32)
$\sum \dots \dots () \dots$	o $\frac{3}{8} \frac{L^2-1}{L^2} A_{\text{HT}}(L)$	See (33)
$\sum \dots \dots ()_2 \dots$	e See (34)	
$\sum \dots \dots ()_2 \dots$	o See (35)	

For periodic systems we conjecture that the components  $\psi^P(L, s, t)$  defined as

$$\psi^P(L, s, t) = (()_s)_t)_{(L/2)-s-t} \quad \text{for even } L \tag{19}$$

$$\psi^P(L, s, t) = (()_s)_t)_{((L-1)/2)-s-t}| \quad \text{for odd } L \tag{20}$$

are given as the coefficient of  $x^s$  of the polynomial:

$$\det_{1 \leq i, j \leq s+t} \left[ \binom{i+j-2+L-2s-2t}{i-1} + x\delta_{i,j} \right]. \tag{21}$$

For even reflecting systems this vector element, denoted as  $\psi^R(L, s, t)$ , is conjectured to be [30]

$$\begin{aligned} \psi^R(L, s, t) &= \det_{1 \leq i, j \leq s} \left[ \binom{L+j-2i}{s+t-j} - \binom{L+j-2i}{s+t-j-2i+1} \right] \\ &= \left[ \prod_{j=1}^s \frac{(j-1)!(L-2s+2j-1)!(L-2s-2t+3j-1)!}{(L-t-s+2j-1)!(t+s-j)!(L-2s-2t+2j-1)!} \right. \\ &\quad \left. \times \frac{(L-s+t+2j-1)!}{(L-2s+t+3j-1)!} \right]. \end{aligned} \tag{22}$$

For odd reflecting systems we have less general results. The above formula for  $\psi^r(L, s, t)$  gives for  $s + t = (L - 1)/2$  the vector element  $(\cdot)_s |(\cdot)_t$ . We conjecture that the vector element  $(\cdot)_r |(\cdot)_t$  is given by

$$\binom{2r + 2t + 1}{r} - \binom{2r + 2t + 1}{r - 3}. \tag{23}$$

The vector element  $(\cdot)_r |(\cdot)$  is given by

$$\sum_{k=1}^{r+1} \frac{1}{k + 1} \binom{2k}{k}. \tag{24}$$

In the special cases of the vector elements  $\psi(L, 1, 1)$  and  $\psi(L, 2, 1)$ , it is possible to prove the expressions that follow from the above formula using elementary manipulations involving the Hamiltonian. We illustrate this for an even periodic system. According to (21),  $\psi^p(L, 1, 1) = L - 1$ . Let the connectivity states on which the loop Hamiltonian  $H$  defined in (2) acts be denoted as ket vectors. We can then write

$$\langle \phi | H^\dagger |(\cdot)_{L/2} \rangle = 0 \tag{25}$$

where  $|\phi\rangle$  is the eigenvector. Since

$$H^\dagger |(\cdot)_{L/2} \rangle = -|((\cdot))_{L/2-2} \rangle + (L - 1)|(\cdot)_{L/2} \rangle \tag{26}$$

it follows that the vector element  $\psi^p(L, 1, 1)$  has indeed the value  $L - 1$ .

#### 4.2. Open and mixed boundary conditions

For mixed and open boundary conditions the vector element consisting of a sequence of  $L$  lines ending at the left boundary,  $\cdot)_L$  is the smallest component. In the case of the mixed boundary condition all components are conjectured to be integers after normalizing the smallest component to unity. For open boundary conditions we define the coprime integers  $V(L)$  and  $W(L)$  by

$$\frac{V(L)}{W(L)} = \frac{A_V(L + 1)}{A_V(L + 3)}, \tag{27}$$

for even  $L$ , and for odd  $L$

$$\frac{V(L)}{W(L)} = \frac{N_8(L + 1)}{N_8(L + 3)}. \tag{28}$$

We conjecture that all components are integers when the smallest component is normalized to  $V(L)$ . In table 2 we have listed the components for which we conjecture analytical expressions. The largest component for even mixed systems is a sequence of  $L/2$  minimal one-nests,  $(\cdot)^{L/2}$ . The value of this component is given as  $A_V(L + 1)^2$ . For even open systems the largest component is  $\cdot)^{(L-2)/2}$  (and its value is conjectured in [12] to be

$$V(L) \left[ \frac{A_V(L + 3)N_8(L)R(L/2, L + 2)}{A_V(L + 1)} - A_V(L + 1)R(L/2, L + 3) \right]. \tag{29}$$

For an odd system the largest component is given by a line connected to the left boundary placed to the left of a sequence of minimal one-nests,  $\cdot)^{(L-1)/2}$ . For mixed systems these components are given as  $A_V(L)A_V(L + 2)$ , and for open systems they are given as  $V(L)R((L - 1)/2, L + 2)A_V(L + 2)$ . The sum of all components is given by  $A_{HV}(2L + 3)$  for mixed systems, and  $V(L)A_{HV}(2L + 5)$  for open systems.

**Table 2.** Components of the eigenvector for mixed and open boundary conditions.

Component	Mixed	Open
$)_L$	1	$V(L)$ , see (27) and (28)
$()_{L/2}$	$A_V(L+1)$	$V(L)N_8(L+2)$
$()_{(L-1)/2}$	$N_8(L+1)$	$V(L)A_V(L+2)$
$()^{L/2}$	$A_V(L+1)^2$	$V(L)R\left(\frac{L}{2}, L+2\right)N_8(L+2)$
$()^{(L-1)/2}$	$A_V(L)A_V(L+2)$	$V(L)R\left(\frac{L-1}{2}, L+2\right)A_V(L+2)$
$()^{(L-2)/2}(\dots)$		See (29)
$((^n)_{m-n})_{L-2m}$	$R(n, L+1)R(m+1, L+1)$	$V(L)R(n, L+2)R(m+1, L+2)$
$()_{(L-1)/2}$	$A_V(L+2)$	
$)()_{(L-2)/2}$	$A_V(L+1)\frac{6}{L+4}\binom{L}{(L-2)/2}$	
$()()_{(L-2)/2}$	$A_V(L+1)\left[\binom{L-1}{L/2}-\binom{L-1}{(L+6)/2}\right]$	
$()_{(L-2)/2}()$	$A_V(L+1)\sum_{k=1}^{L/2}\binom{2k}{k}$	
$)()^{(L-2)/2}$	$A_V(L+1)^2$	
$\sum \dots \dots$	$A_{HV}(2L+3)$	$V(L)A_{HV}(2L+5)$
$\sum \dots \dots)_n$	See (44)	See (46)

JSTAT (2004) P09010

### 5. Correlations and exponents

In this section we present a number of conjectured expressions for correlations. All conjectured correlations are also listed in tables 1 and 2 where we give the corresponding sums of vector elements. The probability for a minimal one-nest in an even periodic system is

$$\frac{3}{8} \frac{L^2}{L^2 - 1}. \tag{30}$$

For odd periodic systems this probability is

$$\frac{3}{8} \frac{L^2 - 1}{L^2}. \tag{31}$$

In a reflecting system, the probability of a minimal one-nest depends on its position. The average of this quantity over all positions for an even reflecting system is

$$\frac{3L^2 + 2L + 4}{(L - 1)(8L + 4)}. \tag{32}$$

For an odd reflecting system this average is given as

$$\frac{3L + 5}{8L + 4}. \tag{33}$$

The probability for a minimal two-nest in an even periodic system is

$$\frac{(L-2)(59L^5 + 118L^4 - 44L^3 - 88L^2 + 5760L - 28\,800)}{2^{10}(L^2-9)(L^2-1)^2}. \quad (34)$$

And for an odd periodic system it is

$$\frac{(L-3)(59L^6 + 531L^5 + 1460L^4 - 750L^3 + 3949L^2 - 20\,001L - 1890)}{2^{10}(L-2)L^3(L+2)^2(L+4)}. \quad (35)$$

Because for many correlations the asymptotic large  $L$  dependence is algebraic with a nontrivial exponent, we give this behaviour using the symbol  $\propto$ . The probability for a maximal  $m$ -nest in even periodic systems is

$$\frac{Q((L/2) - m, L + 1)}{A_{\text{HT}}(L)} \propto L^{-(1+m)(1+2m)/3} \quad (36)$$

and for odd periodic systems this probability becomes

$$\frac{Q(((L-1)/2) - m, L + 1)}{A_{\text{HT}}(L)} \propto L^{-(1+m)(3+2m)/3}. \quad (37)$$

The probability for a maximal  $m$ -nest in an even reflecting system is

$$\frac{R((L/2) - m, L + 1)}{A_{\text{V}}(L + 1)} \propto L^{-(2/3)m(m+1)}. \quad (38)$$

For an odd reflecting system this probability is

$$\frac{R(((L-1)/2) - m, L + 1)}{N_8(L + 1)} \propto L^{-(2/3)(m+1)^2}. \quad (39)$$

In an even periodic system the probability  $P(L, n)$  that  $n$  consecutive points are disconnected from each other is given as

$$P(L, n) = \frac{S(L, n)}{S(2n, n)A(n)} \quad (40)$$

where  $S(L, n)$  for even  $n$  is given as

$$\frac{\prod_{p=1}^{n/2} \prod_{k=p}^{2p-1} (L^2 - 4k^2)}{\prod_{p=0}^{n/2-1} (L^2 - (2p+1)^2)^{n/2-p}} \quad (41)$$

while for odd  $n$  it is

$$\frac{\prod_{p=2}^{(n+1)/2} \prod_{k=p}^{2p-2} (L^2 - 4k^2)}{\prod_{p=0}^{(n-3)/2-1} (L^2 - (2p+1)^2)^{(n-1)/2-p}}. \quad (42)$$

The function  $f(n) \equiv \lim_{L \rightarrow \infty} P(L, n)$  has the following asymptotic behaviour for large  $n$ :

$$f(n) \propto 4^{-n(3n+2)/4} (3\sqrt{3})^{n(n+1)/2} n^{7/72}. \quad (43)$$

For mixed and open boundary conditions we have obtained the probability that at least the  $n$  rightmost sites are connected to the left boundary. For mixed boundary

conditions, we conjecture that the sum of the corresponding vector elements  $P_{\text{mx}}(L, n)$  is given as

$$P_{\text{mx}}(L, n) = R\left(\left\lfloor \frac{L-n+1}{2} \right\rfloor, L+1\right) R\left(\left\lfloor \frac{L-n+2}{2} \right\rfloor, L+2\right). \quad (44)$$

The probability decays as

$$\frac{P_{\text{mx}}(L, n)}{P_{\text{mx}}(L, 0)} \propto L^{-n(1+n)/3}. \quad (45)$$

For open boundary conditions, the sum of vector elements in which at least the  $n$  rightmost lines are connected to the left boundary is conjectured to be

$$P_{\text{op}}(L, n) = V(L) R\left(\left\lfloor \frac{L-n+1}{2} \right\rfloor, L+2\right) R\left(\left\lfloor \frac{L-n+2}{2} \right\rfloor, L+3\right). \quad (46)$$

The normalized probability decays as

$$\frac{P_{\text{op}}(L, n)}{P_{\text{op}}(L, 0)} \propto L^{-n(3+n)/3}. \quad (47)$$

## 6. Fully packed loop diagrams

As we have indicated above, the sum of the components of the eigenvector of the transfer matrix of the dense O(1) loop model is conjectured to be the number of ASMs of a certain symmetry class. The specific symmetry class is determined by the boundary condition of the O(1) loop model. In this section this connection will be specified further.

It is known (see e.g. [7]) that ASMs are in bijection with certain classes of fully packed loop (FPL) diagrams on square grids. A grid is a rectangular section of the square lattice, of which all vertices are incident on four edges, and on each edge one or two vertices are incident. The edges on which only one vertex is incident are called external or boundary edges. An FPL diagram on a grid is a collection of lattice paths such that each vertex is visited once by one of the paths. Each of the paths is cyclic or open. In the latter case it runs from an external edge to another external edge. For later reference we number the external edges anticlockwise starting with the uppermost horizontal edge on the left side of the grid. Figure 8 shows an example of an FPL diagram on a square grid.

The mapping between FPL diagrams and ASMs is symmetry preserving. The conjectured equality between the sum of the components of the eigenvector and the number of ASMs of certain symmetry thus extends to the number of FPL diagrams of the same symmetry. Consider FPL diagrams on a square grid in which the even-numbered external edges are visited by the paths. By the connectivity of the FPL diagram we denote the way in which these external edges are pairwise connected by the paths. Razumov and Stroganov [3] conjectured that the components of the ground-state eigenvector of the O(1) loop model with periodic identified boundaries are equal to the number of  $L/2 \times L/2$  FPL diagrams with the corresponding connectivity. This connection was later generalized to other boundary conditions: periodic unidentified boundaries [4] to the class of half-turn invariant FPL diagrams, reflecting boundary conditions [9] to vertically symmetric FPL diagrams. Here we generalize it to open and mixed boundary conditions. The latter has already been reported in [11].

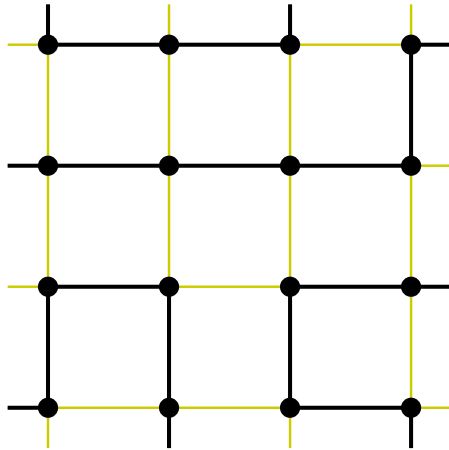


**Figure 8.** An FPL diagram.

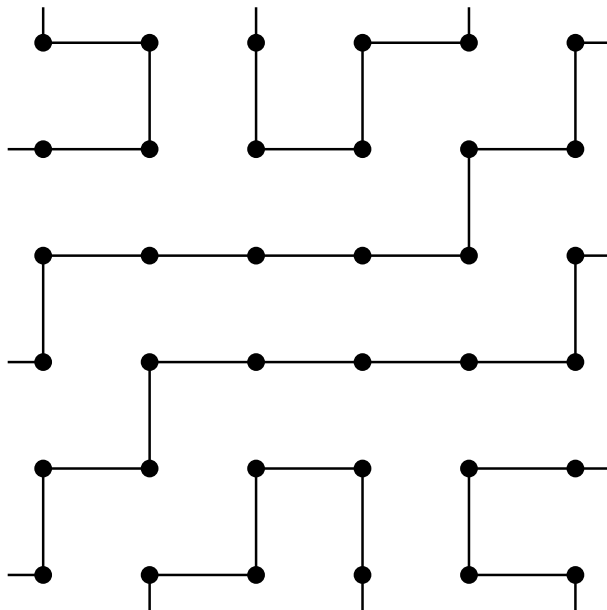


**Figure 9.** Half-turn invariant FPL diagram corresponding to the vector element  $(\text{()})$ .

The case of periodic unidentified boundaries maps into the class of half-turn invariant FPL diagrams on an  $L \times L$  grid; see figure 9 for an example. Again only even-numbered external edges are visited. They represent a row of vertical edges of the  $O(1)$  loop model.

- *Reflecting boundaries.* The eigenvector components of the  $O(1)$  loop model on a strip with even size  $L$  and reflecting boundary conditions map onto a vertically symmetric FPL diagram on a  $(L + 1) \times (L + 1)$  grid. This symmetry indicates that the FPL configurations are completely determined by the  $L/2 \times (L + 1)$  rectangle. Let the long sides of the rectangle be horizontal, then external edges of the top side are not visited by the paths. Of the remaining three sides the even-numbered edges are visited. The number of these FPL diagrams with a given connectivity is conjectured to be the

component of the eigenvector with that connectivity. Because in the  $L/2 \times (L + 1)$  geometry the path configuration at the left and right sides is completely fixed, it is sufficient to specify only an  $L/2 \times (L - 1)$  rectangle, with now the odd-numbered external edges visited.

A very similar conjecture has been given for an odd-sized system with reflecting boundaries. Here the rectangle is  $(L - 1)/2 \times L$ , again oriented with the long sides horizontal. Of the top side (of size  $L$ ) precisely one of the external edges is visited, and of the other sides the odd-numbered edges. One of the latter is connected to the exceptional top side edge, and represents the unpaired site of the O(1) model.

- *Mixed boundary conditions.* When one boundary of the O(1) strip is reflecting and the other is open, the sum of the ground state vector elements we conjecture to be equal to the number of horizontally and vertically symmetric  $(2L + 3) \times (2L + 3)$  FPL diagrams (see also [11]). Again the symmetry prescribes that one quadrant of the grid completely determines the configuration. An example is shown in figure 10. The configuration at the boundary sites is also determined by the requirement that all sites be visited by the paths. As a result the eigenvector corresponds to the FPL diagrams on an  $L \times L$  grid. Of the left and bottom sides the even-numbered external edges are visited, and all of the top side. The left and bottom sides represent the sites of the O(1) vector. Those of the top side represent the open boundary. The connectivity is defined by the way the left and bottom edges are mutually connected, and by which of them are connected to any edge of the top side. We conjecture the number of FPL diagrams with a given connectivity to be equal to the eigenvector element with the corresponding connectivity.
- *Open boundaries.* When the O(1) loop model has two open boundaries, one may or may not distinguish these boundaries in defining the connectivity. In the data presented above we do make the distinction if a site is connected to the right or the left boundary. For this case we do not have conjectures to connect the individual vector components to FPL counts. We can, however, make the connection when we identify the two boundaries in the definition of the connectivity. For odd system size  $L$  the numbers are derived from the class of vertically symmetric FPL diagrams of size  $(L + 2) \times (L + 2)$ . These are completely specified by the configuration on an  $L \times (L + 1)/2$  rectangle. The external edges of the top side, of size  $L$ , are all visited by the paths. These represent the boundary. Of the remaining sides the odd-numbered external edges are visited, and the connectivity specifies how these are connected to each other. The components of the eigenvector of the O(1) model is conjectured to be the number of FPL diagrams with the corresponding connectivity.

For even system size  $L$  and identified open boundaries we have the following conjecture. Consider FPL diagrams on an  $L \times (L + 1)$  grid. Two adjacent sides represent the boundary. Of these all external edges except the  $(L + 1)$ th one on the long side are visited by the paths. Of the other two sides the even-numbered edges are visited, and represent the row of edges of the O(1) model. The connectivity specifies which of these edges are pairwise connected by the paths and which are connected to the boundary. An example is shown in figure 11. The number of FPL diagrams with a given connectivity is conjectured to be equal to the eigenvector component with the same connectivity. In this case, the smallest element is not equal to one, but is given by  $A_V(L + 1)$ .

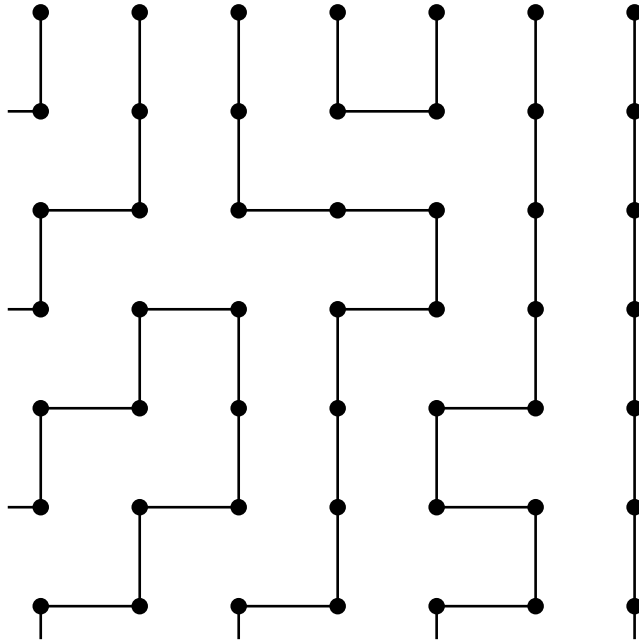


Figure 10. An FPL diagram corresponding to the vector element  $\psi^p(L, s, t)$ .

## 7. Interpretation as families of nonintersecting lattice paths

In this section we will show that the conjectured expressions for the components  $\psi^p(L, s, t)$  and  $\psi^r(L, s, t)$  (see (19), (20) and (22)) enumerate families of nonintersecting lattice paths on finite square lattices. The lattice paths consist of unit steps from points to one of their nearest neighbours. The path may only move in two mutually orthogonal directions, e.g. in the positive  $x$  or negative  $y$  direction.

According to the theorem of Gessel and Viennot on the enumeration of nonintersecting lattice paths [19], we have the following.

Let  $A_1, A_2, \dots, A_n$  and  $E_1, E_2, \dots, E_n$  be lattice points such that for  $i_1 < i_2$  and  $j_1 < j_2$  any lattice path from  $A_{i_1}$  to  $E_{j_2}$  meets any lattice path from  $A_{i_2}$  to  $E_{j_1}$ . Then the number of families  $(P_1, P_2, \dots, P_n)$  of nonintersecting lattice paths, where  $P_i$  runs from  $A_i$  to  $E_i$ , is given by the determinant:

$$\det_{1 \leq i, j \leq n} Z(A_i \rightarrow E_j) \tag{48}$$

where  $Z(A_i \rightarrow E_j)$  denotes the number of all lattice paths from  $A_i$  to  $E_j$

We will now show that the conjectured expression for  $\psi^p(L, s, t)$  enumerates the total number of  $s$  nonintersecting lattice paths on an  $(s+t) \times (L-s-t)$  square lattice subjected to the following constraints.

- (1) A path is required to start at a point  $(0, k)$  with  $0 \leq k \leq s+t-1$ .
- (2) A path starting at  $(0, k)$  is required to end at the point  $(k+L-2s-2t, 0)$ .

See figure 12 for an example.

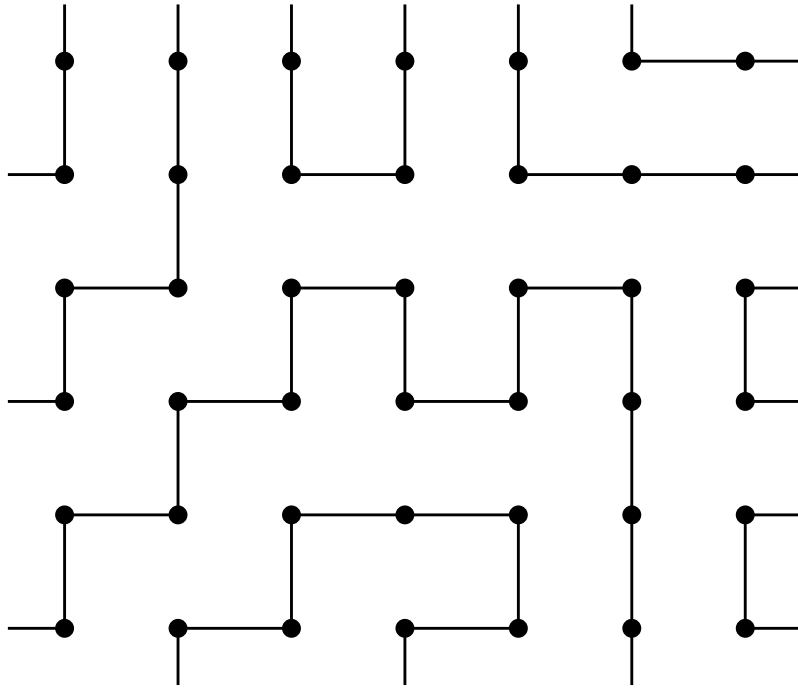


**Figure 11.** An FPL diagram corresponding to the vector element  $||(\cdot)$ .

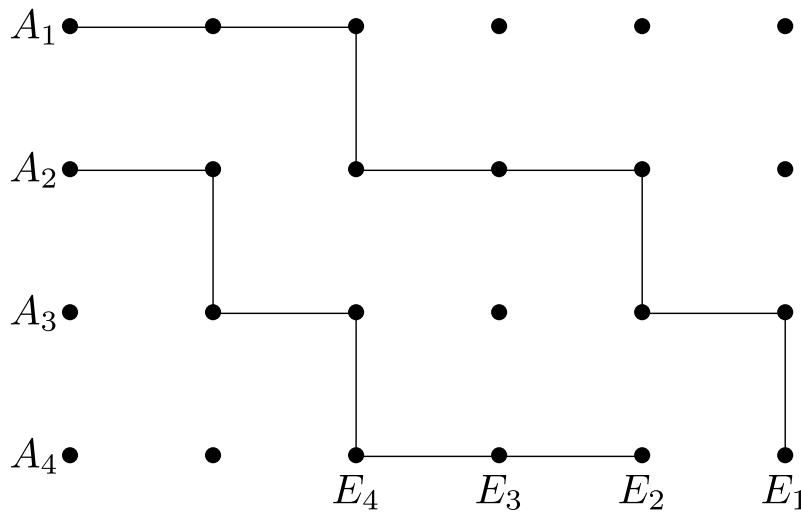


**Figure 12.** A contribution to  $\psi^p(L = 10, s = 2, t = 2)$ . Paths starting at  $A_i$  have to end at  $E_i$ .

Using the theorem of Gessel and Viennot we can write the total number of families of nonintersecting lattice paths subjected to the above constraints as

$$\sum_{0 \leq p_1 < p_2 < \dots < p_{s-1} < p_s \leq s+t-1} \det_{1 \leq i, j \leq s} \begin{pmatrix} p_j + p_i + 2p \\ p_i \end{pmatrix}. \tag{49}$$

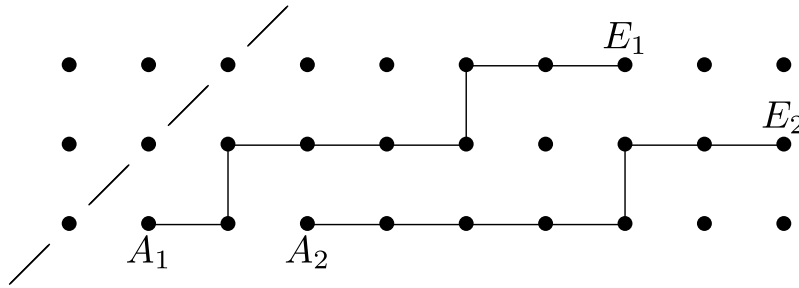


**Figure 13.** A contribution to  $\psi^r(L = 10, s = 2, t = 2)$ . Paths starting at  $A_i$  have to end at  $E_i$  and are not allowed to touch the dashed line.

Note that this is precisely the sum of all  $s$ th order principal minors of the matrix  $M_{i,j} = \binom{i+j+2p}{i}$ , where  $0 \leq i, j \leq s + t - 1$ . In general, the sum of  $s$ th order principal minors of an arbitrary  $n \times n$  matrix will yield the absolute value of the coefficient of  $x^{n-s}$  of the characteristic polynomial of the matrix. It thus follows that the total number of nonintersecting lattice paths is given by the absolute value of the coefficient of  $x^t$  of the characteristic polynomial of the matrix  $M_{i,j}$ .

The conjectured expression for  $\psi^r(L, s, t)$  (22) gives the number of  $s$  nonintersecting lattice paths subjected to the following constraints.

- (1) The  $k$ th path ( $1 \leq k \leq s$ ) starts at the point  $(2k - 1, 0)$  and ends at the point  $(L - s - t + 2k - 1, s + t - k)$ .
- (2) Every path stays below the diagonal line  $(x, x)$ .

See figure 13 for an example.

The proof that the number of families of nonintersecting lattice paths corresponds to the expression (22) is again a straightforward application of the theorem of Gessel and Viennot. From the reflection principle it follows that the total number of paths from the point  $(a, 0)$  to the point  $(m, n)$ , with  $m \geq n$ , that stay below the diagonal line  $(x, x)$  is given by (see e.g. [20])

$$B(a, m, n) = \binom{m + n - a}{n} - \binom{m + n - a}{m}. \tag{50}$$

It thus follows that the total number of families of nonintersecting lattice paths is given as the determinant:

$$\det_{1 \leq i, j \leq s} B(2i - 1, L + r - s - 2t + 2j - 1, r + s - j). \tag{51}$$

Inserting (50) in this determinant yields (22).

## 8. Mapping loop model $\rightarrow$ ground state of $XXZ$ model

In this section we derive the mapping from the dense O(1) loop model to the ground state of the  $XXZ$  model for all the boundary conditions considered in this paper. Proceeding in a similar way as in [22], we first add an extra degree of freedom to the loops of the

dense O(1) model in the form of an orientation. We assign a Boltzmann weight of  $q^{1/4}$  for each left turn and  $q^{-1/4}$  for each right turn. The loopweight thus becomes  $q + q^{-1}$ . The choice  $q = \exp(i\pi/3)$  ensures that this is unity.

In this model a horizontal cut between the vertices is now intersected by arrows. This can be interpreted as a state of a spin chain of length  $L$ . The Hamiltonian of the loop model (2) defines a Hamiltonian acting on the spin chain as follows: the operator  $e_i$  (see figure 5) can be transformed to a spin operator by orienting the two half loops, assigning the correct Boltzmann weights and summing over the orientations. We obtain

$$e_i = (q^{-1/2}|\uparrow\rangle_i|\downarrow\rangle_{i+1} + q^{1/2}|\downarrow\rangle_i|\uparrow\rangle_{i+1})(q^{-1/2}\langle\uparrow|_i\langle\downarrow|_{i+1} + q^{1/2}\langle\downarrow|_i\langle\uparrow|_{i+1}). \quad (52)$$

This expression is indeed compatible with the rules (3). This choice differs from the quantum group convention, in order to avoid a complication in the even periodic system. We can rewrite this in terms of the Pauli matrices as

$$e_i = \frac{1}{2} \left( \sigma_i^x \sigma_{i+1}^x + \sigma_i^y \sigma_{i+1}^y - \frac{1}{2} \sigma_i^z \sigma_{i+1}^z - \frac{i\sqrt{3}}{2} (\sigma_i^z - \sigma_{i+1}^z) + \frac{1}{2} \right). \quad (53)$$

When reflecting boundary conditions are imposed the spin Hamiltonian follows from (5) and (53):

$$H^{\text{ref}} = - \sum_{i=1}^{L-1} \frac{1}{2} \left( \sigma_i^x \sigma_{i+1}^x + \sigma_i^y \sigma_{i+1}^y - \frac{1}{2} \sigma_i^z \sigma_{i+1}^z - \frac{i\sqrt{3}}{2} (\sigma_i^z - \sigma_{i+1}^z) - \frac{3}{2} \right). \quad (54)$$

For periodic boundary conditions we have to distinguish between systems of odd and even lengths. For even periodic systems it is possible for a loop to wind round the cylinder, while for odd periodic systems the presence of the unpaired line will prevent this. Therefore, in case of an odd periodic system, the corresponding  $XXZ$  Hamiltonian is obtained from (53) and (2). We thus obtain

$$H^{\text{odd}} = - \sum_{i=1}^L \frac{1}{2} (\sigma_i^x \sigma_{i+1}^x + \sigma_i^y \sigma_{i+1}^y - \frac{1}{2} \sigma_i^z \sigma_{i+1}^z - \frac{3}{2}). \quad (55)$$

Here  $\sigma_0 = \sigma_L$ .

For an even periodic system, we have to give a unit weight to loops that wind round the cylinder. This can be done by introducing a seam at the boundary between the sites  $L$  and  $1$ . We assign a weight of  $q$  to an arrow pointing from  $L$  to  $1$ , while an arrow pointing in the opposite direction will be assigned a weight of  $q^{-1}$ . As a result  $e_L$  is modified:

$$e_L = (q^{-3/2}|\uparrow\rangle_L|\downarrow\rangle_1 + q^{3/2}|\downarrow\rangle_L|\uparrow\rangle_1)(q^{1/2}\langle\uparrow|_L\langle\downarrow|_1 + q^{-1/2}\langle\downarrow|_L\langle\uparrow|_1). \quad (56)$$

It is convenient to rewrite this in terms of  $\sigma^+$  and  $\sigma^-$ :

$$e_L = \sigma_1^+ \sigma_L^- q^2 + \sigma_1^- \sigma_L^+ q^{-2} - \frac{1}{2} \left( \frac{1}{2} \sigma_1^z \sigma_L^z + \frac{i\sqrt{3}}{2} (\sigma_L^z - \sigma_1^z) - \frac{1}{2} \right). \quad (57)$$

The Hamiltonian is thus given as

$$H^{\text{even}} = - \left[ \sum_{i=1}^{L-1} \frac{1}{2} (\sigma_i^x \sigma_{i+1}^x + \sigma_i^y \sigma_{i+1}^y - \frac{1}{2} \sigma_i^z \sigma_{i+1}^z) - \frac{3}{2} \right] - \sigma_1^+ \sigma_L^- q^2 - \sigma_1^- \sigma_L^+ q^{-2} + \frac{1}{4} \sigma_1^z \sigma_L^z + \frac{3}{4}. \quad (58)$$

To obtain the ground states of the Hamiltonians (54), (55) and (58) from the eigenvectors of the corresponding loop models, one has to assign orientations to all the half loops of the connectivity states contributing to the eigenvectors in all possible ways and assign the correct phase factors. A half loop starting at  $i$  and ending at  $j$  for  $j > i$  corresponds to

$$q^{-1/2}|\uparrow\rangle_i|\downarrow\rangle_j + q^{1/2}|\downarrow\rangle_i|\uparrow\rangle_j. \quad (59)$$

For an even periodic system one has to take into account the presence of the seam. A half loop starting at  $i$  and ending at  $j$  for  $i > j$  that crosses the seam corresponds to the term

$$q^{-3/2}|\uparrow\rangle_i|\downarrow\rangle_j + q^{3/2}|\downarrow\rangle_i|\uparrow\rangle_j. \quad (60)$$

### 8.1. Open and mixed boundary conditions

When open or mixed boundary conditions are imposed, we have to take into account the fact that loops can end at the boundary. We have to give weights to arrows pointing in or out of the left and the right boundary, such that lines starting from one boundary and ending on the same or the other boundary get a unit weight. We denote these weights as  $w_v^d$ , where  $d$  can be  $l$  for the left boundary or  $r$  for the right boundary, while  $v$  can be  $-$  for an arrow pointing into the boundary or  $+$  for an arrow pointing out of the boundary.

Demanding that a line starting from the left boundary and ending on the left boundary has a unit weight yields

$$w_+^l w_-^l \sqrt{3} = 1. \quad (61)$$

Similarly, demanding that a line starting from the right boundary and ending on the right boundary has a unit weight yields

$$w_+^r w_-^r \sqrt{3} = 1. \quad (62)$$

Demanding that a line starting on one boundary ending on the other boundary has a unit weight yields

$$w_+^l w_-^r + w_-^l w_+^r = 1. \quad (63)$$

The choice

$$w_+^l = a3^{-1/4} \quad (64)$$

$$w_-^l = a^{-1}3^{-1/4} \quad (65)$$

$$w_+^r = \frac{a}{2}(3^{1/4} + i3^{-1/4}) \quad (66)$$

$$w_-^r = \frac{1}{2a}(3^{1/4} - i3^{-1/4}) \quad (67)$$

satisfies equations (61)–(63) for general  $a$ .

We can now use these weights to transform the operators  $h_0$  and  $h_L$  (see figure 7) into spin operators. We obtain

$$h_0 = (q^{-1/4}w_-^l|\downarrow\rangle_1 + q^{1/4}w_+^l|\uparrow\rangle_1)(q^{-1/4}w_+^l\langle\downarrow|_1 + q^{1/4}w_-^l\langle\uparrow|_1) \quad (68)$$

$$h_L = (q^{1/4}w_-^r|\downarrow\rangle_L + q^{-1/4}w_+^r|\uparrow\rangle_L)(q^{1/4}w_+^r\langle\downarrow|_L + q^{-1/4}w_-^r\langle\uparrow|_L), \quad (69)$$

acting in the state space of the first and the last spin respectively. We can rewrite this in matrix form as

$$h_0 = \begin{pmatrix} w_+^1 w_-^1 q^{1/2} & (w_+^1)^2 \\ (w_-^1)^2 & w_+^1 w_-^1 q^{-1/2} \end{pmatrix}_1 \quad (70)$$

$$h_L = \begin{pmatrix} w_+^r w_-^r q^{-1/2} & (w_+^r)^2 \\ (w_-^r)^2 & w_+^r w_-^r q^{1/2} \end{pmatrix}_L. \quad (71)$$

The Hamiltonian for mixed boundary conditions (7) can thus be written as

$$H^{\text{mixed}} = - \left[ \sum_{i=1}^{L-1} \frac{1}{2} \left( \sigma_i^x \sigma_{i+1}^x + \sigma_i^y \sigma_{i+1}^y - \frac{1}{2} \sigma_i^z \sigma_{i+1}^z - \frac{i\sqrt{3}}{2} (\sigma_i^z - \sigma_{i+1}^z) - \frac{3}{2} \right) \right] + 1 - h_0 \quad (72)$$

and the Hamiltonian for open boundaries (6) becomes

$$H^{\text{open}} = - \left[ \sum_{i=1}^{L-1} \frac{1}{2} \left( \sigma_i^x \sigma_{i+1}^x + \sigma_i^y \sigma_{i+1}^y - \frac{1}{2} \sigma_i^z \sigma_{i+1}^z - \frac{i\sqrt{3}}{2} (\sigma_i^z - \sigma_{i+1}^z) - \frac{3}{2} \right) \right] + 2 - h_0 - h_L. \quad (73)$$

To obtain the ground states of the Hamiltonians (72) and (73) from the eigenvectors of the corresponding loop models, one proceeds in the same way as in the case of periodic and reflecting systems. A half loop starting at a point  $i$  and ending at a point  $j$  for  $j > i$  produces the term (59). A quarter loop starting at the point  $i$  and ending at the left boundary corresponds to the term

$$q^{-1/4} w_-^1 |\downarrow\rangle_i + q^{1/4} w_+^1 |\uparrow\rangle_i. \quad (74)$$

A quarter loop starting at the point  $i$  and ending at the right boundary corresponds to

$$q^{1/4} w_-^r |\downarrow\rangle_i + q^{-1/4} w_+^r |\uparrow\rangle_i. \quad (75)$$

## 9. Conclusion

We have presented new conjectures for correlations in the dense O(1) loop model on finite by infinite square lattices. We have obtained results for periodic, reflecting, open and mixed boundary conditions. The obtained correlations involve probabilities that points on a row are connected by loops via the half space below the row in certain ways. A conjecture has also been obtained relating the ground state for a system with open identified boundaries to the FPL model on a rectangular grid.

## Acknowledgments

This work was supported by Stichting FOM, which is part of the Dutch foundation of scientific research NWO, and also by the Australian Research Council. We thank Christian Krattenthaler for helping us to find the closed form expression of the determinant in (22) and Pavel Pyatov for correcting an error regarding the largest component of the eigenvector for even open systems.

## Appendix. The boundary term

The Hamiltonian (2) for the periodic system commutes with a whole family of transfer matrices for the percolation or dense  $O(n = 1)$  problem. This is because the Boltzmann weights satisfy the Yang–Baxter equation. The Hamiltonians with a boundary, open or reflecting, also commute with a family of transfer matrices. In this case, besides the Yang–Baxter equation we need the reflection equation [25], which should be satisfied by the boundary weights. In this appendix we study the reflection equation for the dense  $O(n)$  model.

To set the notation we consider the Yang–Baxter equation in the form

$$E_j(u)E_{j+1}(u+v)E_j(v) = E_{j+1}(v)E_j(u+v)E_{j+1}(u) \quad (76)$$

where the operators  $E_j(u)$  are a linear combination of the identity and the monoid  $e_j$ , in a ratio specified by the spectral parameter. The relations (3) among the  $e_j$  are sufficient to show that (76) is solved by

$$E_j(u) = \sin(\lambda - u) + e_j \sin u. \quad (77)$$

This operator suffices to construct the transfer matrix for the periodic system.

The operators  $E$  are also an ingredient of the family of commuting transfer matrices for a system with a boundary. In this case the transfer matrix involves two consecutive rows of vertices [26] of which the horizontal legs are joined at the boundary by a boundary weight, or  $K$ -matrix. The left boundary operator  $F_0(u)$  must satisfy the reflection equation [25]:

$$F_0(u)E_1(u+v)F_0(v)E_1(v-u) = E_1(v-u)F_0(v)E_1(u+v)F_0(u), \quad (78)$$

where now  $F_0(u)$  is a linear combination of the identity and the operator  $h_0$ , which satisfies (4). The coefficient in  $F_0$  of the identity is the weight with which the two legs are simply connected, as in figure 3. The coefficient of  $h_0$  is the weight with which both legs are connected to the boundary. The solution to this equation is given by

$$F_0(u) = A + B \sin(\lambda/2 - 2u) + 2B \cos(\lambda/2) \sin(2u)h_0 \quad (79)$$

for general  $\lambda$ , and arbitrary constants  $A$  and  $B$ . This equation is the central result of this appendix. For the right boundary we have the analogous equation

$$F_L(u)E_{L-1}(u+v)F_L(v)E_{L-1}(v-u) = E_{L-1}(v-u)F_L(v)E_{L-1}(u+v)F_0(u). \quad (80)$$

The trivial solution of (78) is  $B = 0$ , and say  $A = 1$ , in which case  $F_0$  is simply the identity. This corresponds to reflecting boundary conditions, in which the horizontal lines of the double-row transfer matrix are always mutually connected. Since there is no  $u$ -dependence, the Hamiltonian for this case (5) does not have a boundary term.

When  $B$  is nonzero the logarithmic derivative of the transfer matrix will have a term proportional to  $h_0$ . The coefficient of this term is

$$4B \cos(\lambda/2)/[A + B \sin(\lambda/2)].$$

The coefficients of the terms  $e_i$  are equal to  $2/\sin \lambda$ . For  $\lambda = \pi/3$ , the coefficients of  $h_0$  and  $e_i$  are equal when  $A = B$ . This is the case in expressions (6) and (7).

Finally, it is of interest to consider the nature of the boundary of the transfer matrix at the point  $u = \lambda/2$  in which the transfer matrix has left–right reflection symmetry. In the

case of reflecting boundaries,  $B = 0$ , the horizontal lines at the boundary of the even rows are simply connected to that of the odd row below it, as in figure 3. For open boundary conditions we choose  $A$  and  $B$  equal as indicated above. The common magnitude of  $A$  and  $B$  is immaterial and simply multiplies the entire transfer matrix. In the convenient choice  $A = B = 1/2$  at  $\lambda = \pi/3$  the boundary weight can be interpreted as a probability distribution: the coefficient in (79) of  $h_0$  and the identity are  $3/4$  and  $1/4$  respectively, to be interpreted as the probability that the horizontal legs of two consecutive rows are connected to the boundary, or to each other, respectively.

## References

- [1] Stroganov Yu G, 2001 *J. Phys. A: Math. Gen.* **34** L179
- [2] Razumov A V and Stroganov Yu G, 2001 *J. Phys. A: Math. Gen.* **34** 3185
- [3] Razumov A V and Stroganov Yu G, 2004 *Theor. Math. Phys.* **138** 333
- [4] Razumov A V and Stroganov Yu G, 2001 *Preprint cond-mat/0108103*
- [5] Mills W H, Robbins D P and Rumsey H, 1982 *Invent. Math.* **66** 73
- [6] Mills W H, Robbins D P and Rumsey H, 1983 *J. Comb. Ser. A* **34** 340
- [7] Elkies N, Kuperberg G, Larsen M and Propp J, 1992 *J. Alg. Comb.* **1** 111  
Elkies N, Kuperberg G, Larsen M and Propp J, 1992 *J. Alg. Comb.* **1** 219
- [8] Batchelor M T, de Gier J and Nienhuis B, 2001 *J. Phys. A: Math. Gen.* **34** L265
- [9] Pearce P A, Rittenberg V, de Gier J and Nienhuis B, 2002 *J. Phys. A: Math. Gen.* **35** L661
- [10] de Gier J, Nienhuis B, Pearce P A and Rittenberg V, 2003 *Phys. Rev. E* **67** 016101
- [11] de Gier J, 2002 *Preprint math.CO/0211285*
- [12] Pyatov P, 2004 *J. Stat. Mech.: Theor. Exp.* P09003 [[math-ph/0406025](http://arxiv.org/abs/math-ph/0406025)]
- [13] de Gier J, Batchelor M T, Nienhuis B and Mitra S, 2002 *J. Math. Phys.* **43** 4135
- [14] Kuperberg G, 2002 *Ann. Math.* **2** **156** 835
- [15] Kuperberg G, 1996 *Int. Math. Res. Not.* (3) 139
- [16] Robbins D P, 2000 *Preprint math.CO/0008045*
- [17] Zeilberger D, 1996 *E. J. Comb.* **3** R13 84
- [18] MacMahon P A, 1960 *Combinatory Analysis* vol 2 (New York: Chelsea) (Sections 429 and 494)
- [19] Gessel I M and Viennot X, 1985 *Adv. Math.* **58** 300
- [20] Mohanty S G, 1979 *Lattice Path Counting and Applications* (New York: Academic)
- [21] Blöte H W J and Nienhuis B, 1989 *J. Phys. A: Math. Gen.* **22** 1415
- [22] Baxter R J, Kelland S B and Wu F Y, 1976 *J. Phys. A: Math. Gen.* **9** 397
- [23] Wu F Y, 1982 *Rev. Mod. Phys.* **54** 235
- [24] Temperley H N V and Lieb E H, 1971 *Proc. R. Soc. London A* **322** 251
- [25] Sklyanin E K, 1988 *J. Phys. A: Math. Gen.* **21** 2375
- [26] Behrend R E, Pearce P A and O'Brien D L, 1996 *J. Stat. Phys.* **84** 1  
Zhou Y and Batchelor M T, 1996 *Nucl. Phys. B* **466** 488
- [27] Levy D, 1991 *Phys. Rev. Lett.* **67** 1971
- [28] Martin P and Saleur H, 1993 *Commun. Math. Phys.* **158** 155
- [29] See <http://www.research.att.com/~njas/sequences>
- [30] The mathematica procedure rate, implementing this procedure, written by Christian Krattenthaler can be downloaded from <http://www.mat.univie.ac.at/~kratt/rate/rate.html>